Ecological Modelling 336 (2016) 70–81

Contents lists available at ScienceDirect

Ecological Modelling

journal homepage: www.elsevier.com/locate/ecolmodel

North American invasion of Spotted-Wing Drosophila (*Drosophila suzukii*): A mechanistic model of population dynamics

Aaron B. Langille[a,b,*], Ellen M. Arteca[b], Geraldine D. Ryan[a], Lisa M. Emiljanowicz[c], Jonathan A. Newman[c]

[a] School of Environmental Science, University of Guelph, Guelph, Ontario N1G 2W1, Canada
[b] Department of Mathematics and Computer Science, Laurentian University, Sudbury, Ontario P3E 2C6, Canada
[c] Department of Integrative Biology, University of Guelph, Guelph, Ontario N1G 2W1, Canada

ARTICLE INFO

Article history:
Received 18 November 2015
Received in revised form 18 May 2016
Accepted 24 May 2016

Keywords:
Drosophila suzukii
Mechanistic model
Continuous time
Temperature dependent development
Reproductive diapause
Fruit quality

ABSTRACT

Drosophila suzukii is a relatively new threat to the soft-skinned fruit industry in North America. The presence of this pest in North America is a concern and assessing the risk of potential infestation and damage can help guide regional management strategies. We have developed a continuous time stage structured population model parameterized with empirical data based on laboratory observations. The principle environmental driver of vital rates (mortality, fecundity and development) for the model is temperature though our results suggest that reproductive diapause and quality of fruit available to the population may also have significant effect on population size. The model was run with several generalized temperature profiles and various observed temperature data sets for locations known to be important for berry production. While southern regions appear to be most suitable for supporting high population densities due to warm temperatures throughout the year, northern regions with moderate temperatures may also be susceptible due to a lack of extreme cold or heat, both of which limit development and increase mortality.

1. Introduction

Reports of *Drosophila suzukii*, commonly known as Spotted Wing Drosophila, originating from the mainland of Japan have been present since the 1930s (Kanzawa, 1939). However, its rise as a pest of global significance has taken place largely over the past 35 years and in continental North America since circa 2009 (Hauser, 2011). *D. suzukii* has been confirmed or suspected present in countries across all continents except Australia and Antarctica (Asplen et al., 2015) and has a wide range of reported hosts including strawberries, raspberries, blueberries, blackberries, peaches, nectarines, pears, sweet and sour cherries, plums, apricots and both table and wine varieties of grape (Walsh et al., 2011).

D. suzukii is one of only two known species of *Drosophila* that prefer fresh, soft-skinned fruit at or near the stage of optimal harvest ripeness (Lee et al., 2011; Walsh et al., 2011). Females of this species possess a serrated ovipositor that allows them to attack pre-harvest fruit. Early detection of infestation is difficult as the oviposition incision is small and the visible consequences of larval feeding do not immediately appear. Empirical data for North America are not yet readily available but Bolda et al. (2010) provides a benchmark estimate of potential yield losses due to *D. suzukii* infestation at 20%. Based on 2008 harvest yields, this would result in a >$500 million loss in the US states of Washington, Oregon and California alone (accounting for strawberries, blueberries, raspberries, blackberries and cherries only). While the western United States and Canada are important regions for the soft-skinned fruit industry in North America there are other regions that are likely to be concerned about the spread and impact of *D. suzukii*.

Due to its potential to cause significant economic losses in many areas of North America and the need to establish effective pest management strategies, we developed a mechanistic, continuous time mathematical model with overlapping generations. Wherever possible, the model has been parameterized using experimental and observational data on *D. suzukii* life history (see Emiljanowicz et al., 2014; Ryan et al., 2016, for further information).

We have two principle objectives in constructing this model: (i) to gain a better understanding of the temporal and spatial patterns of *D. suzukii* population growth, and hence risk, that result from particular assumptions about crucial mechanisms; and (ii) to create a useful tool for answering interesting "what if" questions regarding *D. suzukii* invasion, climate and climatic change.

* Corresponding author at: Department of Mathematics and Computer Science, Laurentian University, Sudbury, Ontario P3E 2C6, Canada.
E-mail address: alangille@cs.laurentian.ca (A.B. Langille).

http://dx.doi.org/10.1016/j.ecolmodel.2016.05.014
0304-3800/

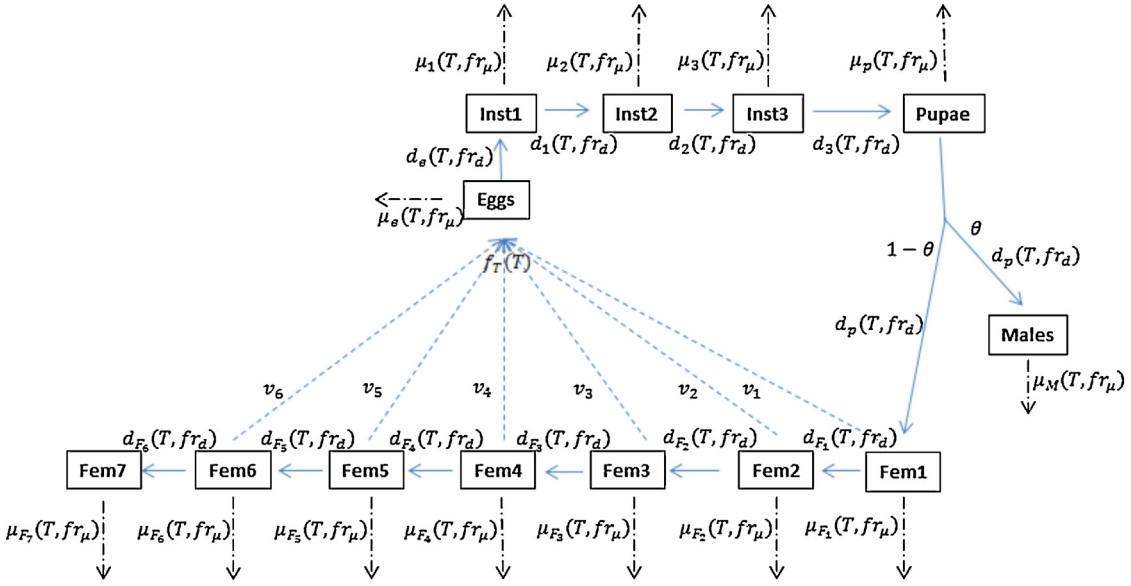

Fig. 1. Schematic of the modelled population stage structure and relationships between state variable equations including principal input and output parameters. Most development and mortality processes are temperature (T) dependent and rely on the fruit submodel (fr) when included. Here mortality is represented as the sum of intrinsic and extrinsic factors (see main text).

A mechanistic model can help us to meet both of these objectives. Mechanisms are a critical part of biological understanding. "What if" questions usually involve changes in the environment, autecology, or synecology of the organism. These questions require changes to the model system that are not readily accommodated in non-mechanistic approaches.

By mechanistic we mean that the model is based upon what we think are the most important mechanistic processes that determine population dynamics. Such models are particularly useful because they allow any model prediction to be traced back to the process(es) that most influences it. Since mechanistic models often have many parameters, all of which are tunable, our goal is only to achieve satisfactory quantitative behavior. Our goal is not forecasting, for which statistical models are often better suited (see e.g., Thornley and France, 2007; for further discussion).

1.1. D. suzukii *life history*

D. suzukii develop through the following stages (with average duration reported in days based on laboratory diet and at a constant temperature of 22 °C): egg (1.4 d), three larval instars (6 d total), pupae (5.8 d), and adult (72 d) (see Emiljanowicz et al., 2014; for details).

Various *Drosophila* species are subject to a reproductive diapause regulated primarily by photoperiod and temperature (Ohtsu et al., 1993). As the number of hours of daylight decreases, reproduction ceases for several species (Saunders et al., 1989; Kimura, 1990). According to Saunders et al. (1989) diapause may be terminated by either an increase in the number of daylight hours, or more importantly for temperate regions, an increase in temperatures (approximately 18 °C for *Drosophila melanogaster*). It has been suggested that *D. suzukii* also experiences a reproductive diapause. Mitsui et al. (2010) found that populations of *D. suzukii* in central Japan had reproductively mature ovaries during summer months, while ovaries were underdeveloped for females trapped in colder months. However, to the best of our knowledge, the specific details of diapause induction and termination have not been elucidated for this species.

D. suzukii experiences both intrinsic and extrinsic mortality. Intrinsic mortality rate is the per capita rate of mortality assumed to be the result of biological aging. It can be contrasted with extrinsic mortality which is assumed to be the result of environmental hazards such as natural enemies (predators, parasites and pathogens). Intrinsic mortality rates have been estimated in the lab (Emiljanowicz et al., 2014) under optimal conditions. These rates are not likely to be density dependent, at least in the field; but field-based rates are difficult to estimate. Similarly, extrinsic mortality rates are exceedingly difficult to estimate, at least in the field, which are arguably the only meaningful estimates of these rates.

D. suzukii vital rates are known to be temperature dependent, and development rates may also depend upon host fruit quality (Burrack et al., 2013; Lee et al., 2015). In the laboratory, optimal development rates occur at 28.2 °C (Ryan et al., 2016; Tochen et al., 2014). Optimal fecundity rates occur at 22.9 °C (Ryan et al., 2016; Tochen et al., 2014). The lower and upper developmental thresholds occur at 8 °C and 31 °C (Ryan et al., 2016) and 7.2 °C and 42.1 °C (Tochen et al., 2014). While the results are similar for most observations, we used the estimates provided by Ryan et al. because they were based on experiments that used a finer temperature scale, which, in particular, captured the upper developmental threshold rather than extrapolating it from the fitted curve as Tochen et al. did.

In terms of winter survival, Dalton et al. (2011) conducted laboratory experiments and found that acclimated adult *D. suzukii* can survive for up to 88 days in 10 °C temperatures including a seven day freeze period (from day 18 to day 25) but that adult longevity decreases as temperature decreases. Pupae can survive for 103 days at 10 °C including the seven day freeze period. Their results also suggest that *D. suzukii* is rendered sterile at these low temperatures. They conclude that few individuals are likely to survive the relatively moderate winters of the Pacific Northwest. More recently, Jakobs et al. (2015) found that 80% of control specimens died after 1 h of exposure to cold temperatures (−7 °C) and similar mortality rates were observed after a few days at 0 °C (70–90 h). Survivorship improved with cold acclimation and under fluctuating temperatures but, similar to the work of Dalton et al. (2011) they conclude that *D. suzukii* is not well-adapted to survive temperate winters based on phenotypic characteristics alone. These results suggest that the presence of *D. suzukii* in climates with longer, colder winters is likely due to a combination of overwintering in man-made

habitats, seasonal dispersal from warmer climates and developmental plasticity (but see Stephens et al. (2015) on the presence of winter-morphs). Due to the uncertainty that remains in how *D. suzukii* is overwintering in specific, particularly harsher climates, we do not model beyond a calendar year. As further details become available the model could be extended to include specific overwintering consideration.

2. Model

Population dynamics are represented by a system of coupled linear differential equations. The model presented here is a mechanistic population dynamics model based on the life stages of *D. suzukii*. There are 13 state variables: eggs, three juvenile instars, pupae, adult males and adult females. The adult female population is divided into seven separate sub-stages in order to account for an observed decline in egg viability rates with age. The principal driving variable in the model is temperature as it is demonstrably related to the main population growth processes of fecundity, development and mortality. Wherever possible, parameters have been tuned and equations fit to approximate observed laboratory population dynamics, exceptions to this are noted in the text. A schematic diagram of the model processes is shown in Fig. 1 and a summary of all model parameters and variables is available in the supplementary material.

2.1. Fecundity rate

Our laboratory experiments show that fecundity is dependent on temperature. We used a polynomial function with compact support (i.e., the function is both closed and bounded), similar to that described by Saryazdi and Cheriet (2007), to fit to the experimental data. This function is Gaussian-like, but unlike a Gaussian function, which is defined on the interval $[-\infty, +\infty]$, this function is constrained over a fixed interval [10, 30] where 10 °C and 30 °C were the lowest and highest temperatures respectively where fecundity was observed to be non-zero (Ryan et al., 2016).

$$f_T = \begin{cases} \alpha\left[\dfrac{\gamma+1}{\pi\lambda^{2\gamma+2}}\left(\lambda^2 - \left([T-\tau]^2+\delta^2\right)\right)^{\gamma}\right] & \text{if } T^2+\delta^2 < \lambda^2 \quad \text{and} \quad T_{f,\min} < T < T_{f,\max} \\ 0 & \text{otherwise} \end{cases} \tag{1}$$

where f_T is per capita eggs/day, $T_{f,\max} = 30\,^{\circ}\text{C}$, $\lambda = 52.68\,^{\circ}\text{C}$, $\delta = 5.88\,^{\circ}\text{C}$ and $\tau = 23.26\,^{\circ}\text{C}$ and the dimensionless shape parameters are given by: $\alpha = 676.0$, $\gamma = 88.38$ (see Supplemental Fig. S1; *cf.* Saryazdi and Cheriet for details regarding the constraint conditions on this function). It should be noted that the data used in the fecundity equations and parameters did not distinguish between female and male sterility.

We include the potential for a reproductive diapause through Eqs. (2) and (3). Diapause data from Kimura (1990) including *Drosophila auraria, Drosophila* biauraria, *Drosophila* subauraria, and two geographic strains, *Drosophila* triauraria OI and *Drosophila* triauraria ON, was used to fit a generalized logistic function whereby $F_D(h)$ provides the proportion of females currently in reproductive diapause based on photoperiod in hours, h, at the current time step:

$$F_D(h) = \left(A + \frac{K-A}{\left(1+Q_e^{Bh}\right)^{v}}\right) \times 100^{-1} \tag{2}$$

with dimensionless shape parameters fit to $A = 0.04$, $K = 99.8$, $v = 0.813$, $Q = 3.23 \times 10^{-16}$ and $B = 2.87$ per hour.

The following equations ensure that diapause is terminated by an upper critical temperature (T_D) and is induced according to the number of daylight hours (h_D).

$$S_{1,t+dt} = \begin{cases} 0 & \text{if } s_{1,t} \times s_{2,t} > 0 \text{ and } h < h_D \\ 1 & \text{if } s_{2,t} = 0 \text{ and } T > T_D \\ s_{1,t} & \text{otherwise} \end{cases}$$
$$S_{2,t+dt} = \begin{cases} 0 & \text{if } s_{1,t} = 0 \\ 1 & \text{if } h \geq h_D \\ s_{2,t} & \text{otherwise} \end{cases} \tag{3}$$

where s_1 and s_2 have no biological meaning; rather they act as computational control "switches" to enable and disable diapause, where $h_D = 10$ (hours of daylight) and $T_D = 18\,^{\circ}\text{C}$. We consider both values to be conservative estimates based on a review of the literature on diapause induction and termination of various Drosophilid species. Eqs. (2) and (3) are combined to determine a diapause-related fecundity factor:

$$f_D(h,T,t) = \begin{cases} 0 & \text{if } s_1 = 0 \\ 1 - F_D(h) & \text{otherwise} \end{cases} \tag{4}$$

Eq. (4) returns the proportion of females *not in* reproductive diapause. Overall fecundity (per capita eggs/day) is calculated using Eqs. (1) and (4) as:

$$f = f_T f_D \tag{5}$$

2.2. Juvenile development rate

In order to express the temperature-dependent development of the egg-to-pupal stage, a function similar to one presented in Briere et al. (1999) was fit to experimental laboratory data (Ryan et al., 2016).

$$\check{d}_i = m_i\left(aT(T-T_L)(T_U-T)^{\frac{1}{2}}\right) \tag{6}$$

where $a = 0.0001113$ is a dimensionless shape parameter, and where T is the air temperature (°C), $T_L = 8.0139\,^{\circ}\text{C}$ is the lower temperature threshold, and $T_U = 30.99\,^{\circ}\text{C}$ is the upper temperature threshold. The multipliers m_i are the reciprocal of the number of days (days^{-1}) required to develop from one stage to the next ($m_e = 0.104$, $m_1 = 0.082$, $m_2 = 0.112$, $m_3 = 0.231$, $m_p = 0.470$, where the subscripts denote: eggs, instar 1, instar 2, instar 3 and pupae, respectively) and are used to scale the stage specific development accordingly. As experimental data were available only for the combined egg-to-pupal stage we used the stage-specific development time in constant (optimal) temperature to determine the fraction of time spent in each stage. We then applied those fractions to the temperature dependent egg-to-pupal data to estimate the time spent in the intermediate stages.

2.3. Temperature-dependent mortality

The state variable equations include daily per capita mortality estimated from intrinsic and extrinsic causes. The equation

below is minimized at optimal temperature and is an appropriate shape to approximate mortality from intrinsic causes including temperature-induced mortality.

$$\mu_i = \begin{cases} \sum_{j=0}^{3} \beta_{i,j}(T-\tau)^j & \text{if } T_{\min,\mu} \le T \le T_{\max,\mu} \\ \mu_{i,\max} & \text{otherwise} \end{cases} \quad (7)$$

where i denotes the life stage and j is an exponent ranging from 0 to 3 representing the linear, quadratic and cubic effects of temperature, $\beta_{i,1} = -0.008$, $\beta_{i,2} = 0.00032$, $\beta_{i,3} = -0.000002$, $\tau = 8.178$, $T_{\min,\mu} = 3.0$ (°C) and $T_{\max,\mu} = 33.0$ (°C). τ is a horizontal shift and $\beta_{i,0}$ is a vertical shift of the polynomial. $T_{\min,\mu}$ and $T_{\max,\mu}$ are the temperature thresholds beyond which mortality is maximized and$\mu_{i,max}$ represents the maximum per capita daily intrinsic mortality. $\beta_{i,0}$ and $\mu_{i,\max}$ are stage-specific parameters estimated using non-linear regression from Emiljanowicz et al. (2014) and are listed in Table 1.

In the absence of an empirical estimate for the $\mu_{i,\max}$ values, we assumed that these were equal to three times their corresponding values estimated at constant optimal temperature. We evaluated the sensitivity of the model results to this assumption and found that the results simply scaled to this assumption, but that the resulting dynamics were largely unaffected (see Supplemental Fig. S2).

2.4. Effect of fruit quality on development and mortality

To this point in our presentation, we have assumed that fruit is always available at a quality that maximizes *D. suzukii* development. In order to explore how seasonal fruit availability affects the seasonal population dynamics of *D. suzukii* we implemented a non-mechanistic model of fruit that captures the general phenomenon and temporal dynamics of the ripening and harvesting of a generalized fruit crop. A differential equation was constructed to simulate this process:

$$\frac{dFr}{dt} = \left(\frac{\omega}{G_{Fr}(T)} - D_{Fr}\right) Fr \quad (8)$$

$$Fr = \begin{cases} 0.05 & \text{if } Fr > 0.05 \\ 1 & \text{if } Fr > 1 \\ Fr & \text{otherwise} \end{cases}$$

where ω is a dimensionless shape parameter that determines when fruit will be at optimal ripeness and Fr is a dimensionless index ranging from 0.05 to 1 representing the current quality of fruit present (see Fig. 2a). G_{Fr} (Eq. (10)) is the fruit quality development time and D_{Fr} (Eq. (9)) is fruit quality decline rate. Previous studies have shown that *D. suzukii* can subsist on various wild hosts when cultivated fruit is unavailable (Lee et al., 2015; Walsh et al., 2011). As such, we assume that non-preferred fruit is always available during the simulation, albeit at a minimized quality level, by including a lower bound of 0.05 on Fr. Fruit quality D_{Fr} declines after harvest time lag has elapsed and is calculated as:

$$D_{Fr}(t) = \begin{cases} 0 & \text{if } Fr(t - h_{Fr}) < \varphi \\ \gamma & \text{otherwise} \end{cases} \quad (9)$$

where t is time and φ is the maximum fruit quality value. h_{Fr} represents a harvest time lag, that is, the amount of time that passes between when the fruit is at optimal quality and when it is harvested and removed from the simulation. γ is the constant rate of fruit quality decline over time. At this time, fruit development is modeled to be a single-stage (i.e., not stage specific).

Temperature-based fruit development time, G_{Fr}, is based on a phenological degree-day growth model of sour cherries. The double sigmoid fruit growth model of Zavalloni et al. (2006) was used to calculate the number of days required at various temperatures for sour cherries to reach optimal fruit ripeness. These data points were then fit to the following function:

$$G_{Fr}(T) = \frac{1100}{T - T_{base}} + 30 \quad (10)$$

where T_{base} is a vertical asymptote at 4.0 °C representing the base temperature required for the fruit to develop. As temperature increases the time required for the fruit to develop, G_{Fr}, decreases.

We make the simplifying assumption that fruit is always available to the population and that only the quality changes with time. Fruit below optimal host quality decreases the rate of development of the simulated population. We constructed the following index of fruit quality (Eq. (11)) that is used to modify *D. suzukii* development rates (cf. Newman et al., 2003). This equation is mathematically transparent and of the correct general shape, acting as a "switch on" sigmoid controlling the effect of fruit quality on development.

$$fr_d = m_{f_d}\left(\frac{Fr}{Q_{p,f_d,h}}\right)^{n_{f_d}}\left(1+\left(\frac{Fr}{Q_{p,f_d,h}}\right)^{n_{f_d}}\right)^{-1} + 1 - m_{fd}; 0 \le m_{fd} \le 1 \quad (11)$$

where, Fr (Eq. (8)) is the simulated current host fruit quality value and $m_{fd} = 0.75$, $Q_{p,f_d,h} = 0.5$, and $n_{f_d} = 4$ are shape parameters; m_{fd} influences the strength of the fruit quality response, $Q_{p,f_d,h}$ is a half saturation constant and n_{fd} controls the rate of switching (see Fig. 2b). The index (Eq. (11)) ranges from $1 - m_{f_d}$ to 1, and is used to modify *D. suzukii* development (Eq. (6)) as:

$$d_i = \check{d}_i fr_d \quad (12)$$

Similarly, the effect of fruit quality on mortality is calculated using the following "switch-off" sigmoid:

$$fr_\mu = m_{f_\mu}\left(1+\left(\frac{Fr}{Q_{p,f_\mu}}\right)^{n_{f_\mu}}\right)^{-1} \quad (13)$$

where, $m_{f_\mu} = 0.1$, $Q_{p,f_\mu} = 0.5$, and $n_{f_\mu} = 4.0$ are shape parameters; m_{fd} influences the strength of the mortality response, Q_{p,f_μ} is a half saturation constant and n_{f_d} controls the rate of switching (see Fig. 2b). We consider the effect of fruit host quality on mortality to be additional to the mortality due to temperature. This is a phenomenological representation and we consider it to be equivalent across all life stages. fr_μ creates an additional mortality that ranges from 0 when fruit quality is optimal to 1 when fruit quality is minimal. We thus model intrinsic mortality, μ_{in}, as:

$$\mu_{in} = \mu_i + fr_\mu \quad (14)$$

where μ_i is given by Eq. (7).

2.5. Model state equations

The following equations are used to model the rates of change of the population of the various stages of *D. suzukii*'s life history. The rate of change for the egg stage is given by:

$$\frac{dE}{dt} = \left(\sum_{i=1}^{6} f v_i F_i\right) - E\left(\mu_{in,e} + \mu_{ex,e} + d_e\right) \quad (15)$$

where f is fecundity (Eq. (5)), E is the number of eggs at time t, and v_i represents egg viability at a particular adult female (F_i) stage. Data on female age-specific egg viability were obtained from Emiljanowicz et al. (2014). This is depicted in Fig. 3 (see figure caption for details). Egg daily per capita intrinsic mortality, $\mu_{in,e}$, is given by Eq. (14), and egg daily per capita extrinsic mortality, $\mu_{ex,e}$, represents the rate of egg loss due to natural enemies. d_e represents

Table 1
Estimated parameters that vary by stage for temperature-dependent mortality (see e.g., Emiljanowicz et al., 2014). The $\beta_{i,0}$ parameters are dimensionless shape parameters, and the $\mu_{i,\max}$ are per capita daily mortality rates.

i	Eggs	Instar1	Instar2	Instar3	Pupae	Males	F_1	F_2	F_3	F_4	F_5	F_6	F_7
$\beta_{i,0}$	0.160	0.140	0.085	0.086	0.061	0.134	0.069	0.090	0.201	0.051	0.301	0.251	0.330
$\mu_{i,\max}$	0.328	0.269	0.102	0.107	0.030	0.097	0.054	0.120	0.450	0.0	0.750	0.600	0.837

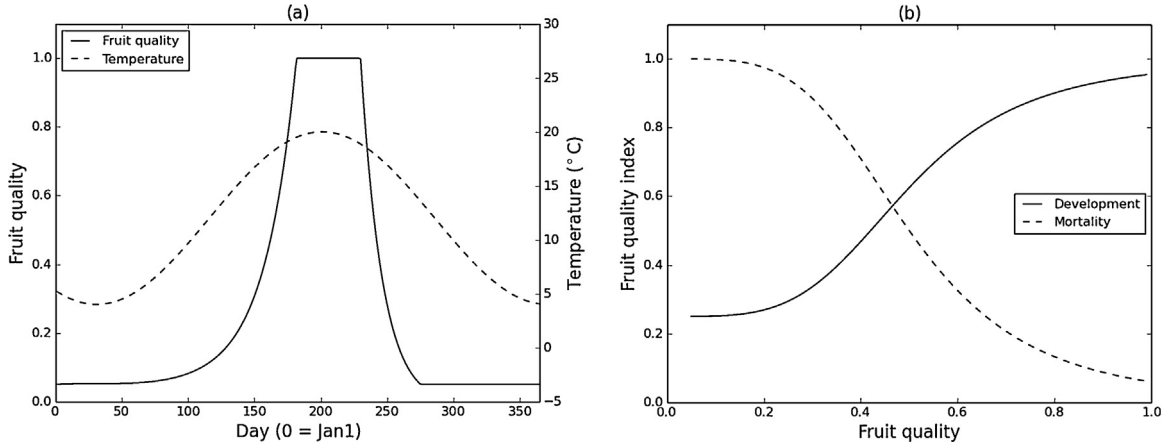

Fig. 2. (a) Fruit quality development time as described in Eq. (8) for a simulated temperature profile (see Section 2.6.2) with a harvest delay, ω, 50. (b) Illustrates fruit quality index (Eq. (11)) for influencing development and fruit quality decline (Eq. (13)) for influencing mortality.

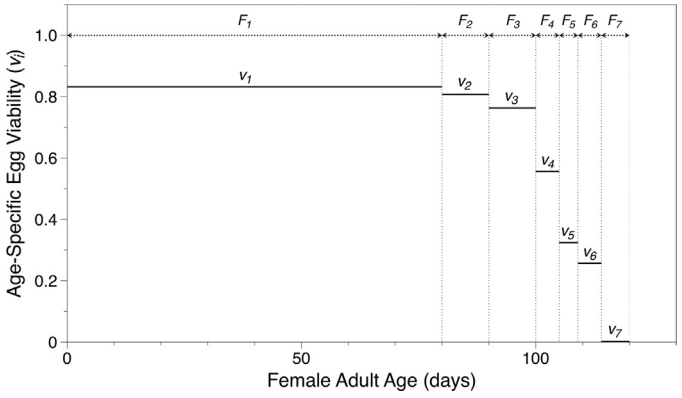

Fig. 3. Female age-specific egg viability. Changes in viability correspond to v_i in Eq. (15) where $v_1 = 0.832$, $v_2 = 0.807$, $v_3 = 0.763$, $v_4 = 0.556$, $v_5 = 0.324$, $v_6 = 0.257$ (see Emiljanowicz et al., 2014 for further information).

the daily per capita rate of eggs developing into first instar larvae (I_1, see Eq. (16)).

The rates of change for each of the three larval instars (I_1, I_2, I_3) are given by:

$$\begin{aligned}\frac{dI_1}{dt} &= d_e E - I_1\left(\mu_{in,1} + \mu_{ex,1} + d_1\right)\\ \frac{dI_i}{dt} &= d_{i-1}I_{i-1} - I_i\left(\mu_{in,i} + \mu_{ex,i} + d_i\right) \qquad \text{for } i = 2,3\end{aligned} \tag{16}$$

again, where $\mu_{in,i}$ and $\mu_{ex,i}$ represent the daily per capita intrinsic and extrinsic mortality rates at each larval instar ($i = 1, 2, 3$) and the d_i represent daily per capita development rates ($i = 1, 2, 3, e$).

The rate of change of the pupal stage is as follows:

$$\frac{dP}{dt} = d_3 I_3 - P\left(\mu_{in,p} + \mu_{ex,p} + d_p\right) \tag{17}$$

where $d_3 I_3$ is the rate of individuals transitioning to pupae from the third instar and $\mu_{in,p}$, $\mu_{ex,p}$ and d_p represent the daily per capita lost to intrinsic mortality (Eq. (14)), extrinsic mortality and development to the adult stage (Eq. (12)), respectively.

The rate of change of adult males is given by,

$$\frac{dM}{dt} = \theta d_p - M\left(\mu_{in,M} + \mu_{ex,M}\right) \tag{18}$$

where $\theta = 0.5$ and represents the proportion of adult flies that are males.

The adult female population is divided into seven substages, each with its own rate of change, to account for declining egg viability as females age (see Fig. 3).

$$\begin{aligned}\frac{dF_1}{dt} &= (1-\theta)d_p P - F_1\left(\mu_{in,F_1} + \mu_{ex,F_1} + d_{F_1}\right)\\ \frac{dF_i}{dt} &= d_{F_{i-1}}F_{i-1} - F_i\left(\mu_{in,F_i} + \mu_{ex,F_i} + d_{F_i}\right) \qquad \text{for } i = 2\ldots7\end{aligned} \tag{19}$$

Pupae develop into adult flies at a daily rate of $d_p P$. The proportion of pupae that become adult female flies (F_1) is $1-\theta$. Different female stages (F_i) were derived from empirical data on female aging and reproductive output (Emiljanowicz et al., 2014) and reflect the female stages over which offspring viability was found to be approximately constant (see Fig. 3). Daily per capita development rates for each of these stages were estimated from laboratory experiments (Emiljanowicz et al., 2014): $d_{F_i} = \frac{1}{80}, \frac{1}{10}, \frac{1}{10}, \frac{1}{5}, \frac{1}{4}, \frac{1}{5}, 0$ for $i = 1$–7. The final adult female stage (F_7) has no development rate as there is no stage beyond F_7 but mortality continues per Eq. (19), and they produce no viable eggs (Fig. 3).

Fig. 1 summarizes the relationship between the differential equations and their principal input and output parameters.

2.6. Environmental equations

2.6.1. Daylength

Equations related to diapause termination (Eqs. (2) and (3)) require number of daylight hours, h, which is calculated as follows (Glarner 2006):

$$h = \frac{24}{\pi} \times \arccos(k') \tag{20}$$

Table 2
Parameters used to generate model temperature profiles per Eq. (23).

Profile name	ε (°C)	k (days^{-1})	s (°lat)	w (°C)	Profile temperature characteristics
Temp A	−17	1.9	13	2	Moderate summer, cold winter, large inter seasonal variation
Temp B	−8	2.15	32	12	Moderate summer, cool winters, moderate inter seasonal variation
Temp C	−6	2.11	36	16.5	Warmer summer, moderate winter, reduced inter seasonal variation
Temp D	−7	1.9	14	22.5	Hot summers, moderate winter, reduced inter seasonal variation

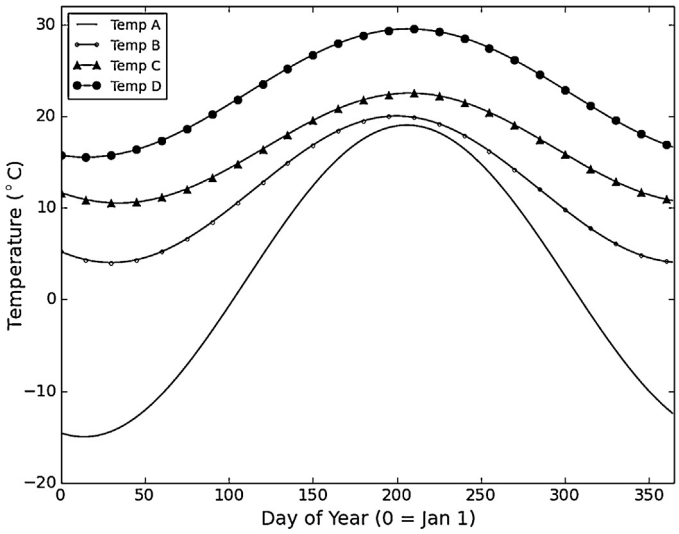

Fig. 4. Modelled temperature profiles approximating 20-year mean daily temperature for Chicoutimi QC (A), Clark county WA (B), Santa Barbara county CA (C) and Hillsborough county FL, (D).

where k' is computed as:

$$k' = \begin{cases} -1 & \text{if } k < -1, \\ 0 & \text{if } k > 1, \\ k & \text{otherwise} \end{cases} \tag{21}$$

Finally, k, the exposed radius between the sun's zenith and the sun's solar circle, is a function of latitude, L, the number of days from January 1st, Y, and the Earth's rotational axis, $R = 23.439°$.

$$k = \tan\left(\frac{\pi L}{180°}\right)\tan\left(\left(\frac{\pi R}{180°}\right)\cos\left(\frac{\pi Y}{182.625°}\right)\right) \tag{22}$$

2.6.2. Daily temperature

In order to demonstrate the base model's behavior we use a cosine model of daily mean temperature (Eq. (23)). For the figures shown in the results section, we parameterized the cosine model to approximate temperature records for four distinct geographical regions across Canada and the United States. The mean 20-year (1993–2013) observed daily mean temperature data for Chicoutimi township, Quebec; Clark county, Washington; Santa Barbara county, California; and Hillsborough county, Florida are reasonably represented by Temp A, B, C and D respectively in Fig. 4 (see also Table 3). Each of these 'profiles' was generated using Eq. (23), where ε, k, s and w represent amplitude (°C), horizontal stretch (days^{-1}), horizontal shift (° latitude) and vertical shift (°C) respectively, and are parameterized as per Table 2.

$$T = \varepsilon \times \cos\left(\frac{k\pi t}{365} - \frac{s\pi}{180}\right) + w \tag{23}$$

Observed mean daily temperature data was collected for a 20-year span (1993–2013) for various soft-skinned fruit producing counties and townships across the United States and Canada (see Table 3). U.S. data was obtained via the National Climatic Data Center (http://www.ncdc.noaa.gov/) and Canadian data was obtained via Environment Canada (http://climate.weather.gc.ca/).

Table 3
Latitude and longitude of 12 of important blueberry and/or strawberry producing counties and townships in the United States and Canada. Sorted by latitude (north–south). See Fig. S3 in Supplemental material for a map of these locations.

County/Township, State/Province	Aproxmimate latitude, longitude
Fraser Valley, BC	49.5800°N, 121.8333°W
Chicoutami, QC	48.4200°N, 71.0500°W
Kent, NB	46.5800°N, 64.8000°W
Cumberland NS	45.7000°N, 64.1000°W
Clark, WA	45.7700°N, 122.4800°W
Norfolk, ON	42.8500°N, 80.2600°W
Allegan, MI	42.5600°N, 86.2500°W
Burlington, NJ	39.8800°N, 74.6700°W
Bladen, NC	34.6200°N, 78.5600°W
Santa Barabara, CA	34.5400°N, 120.0300°W
Wayne, MS	31.6400°N, 88.7000°W
Hillsboro, FL	27.9100°N, 82.3500°W

3. Results

Unless otherwise stated all simulations begin with 10 females (F_1) introduced during the time step for which temperature is adequate to break diapause (18 °C) and are run for a full year starting January 1st. In all results, population counts are limited to females (as the limiting factor) and have been normalized to the largest values in order to emphasize relative rather than absolute differences and to facilitate comparison across time and space. The per-simulation maxima used for normalization as well as a summary of submodel parameters are available in Supplemental material (Tables S1 through S3).

3.1. Base model dynamics

Fig. 5 demonstrates the base population dynamics for a series of simulations where temperature was held constant. Total cumulative population (all adult female stages) over the entire simulation duration is reported and neither diapause nor fruit quality are considered initially. Provided temperatures are favourable for fecundity and development, population size increases exponentially. Cumulative population sizes increase until the optimal temperature is reached, after which development rates decrease, mortality increases and the simulated cumulative population declines. The resulting normalized cumulative population sizes under constant temperature are shown in Fig. 5.

3.2. Effects of starting population size and appearance timing

Since little is known about how *D. suzukii* overwinters and overwintering mortality rates can be decoupled from the actual air temperature by choice of microhabitat or use of heated human-made structures, we examined the sensitivity of the model results to the two principal variables that might vary with overwintering: the size of the population that survives the winter (or immigrates from a region with a warmer climate) and the date at which they

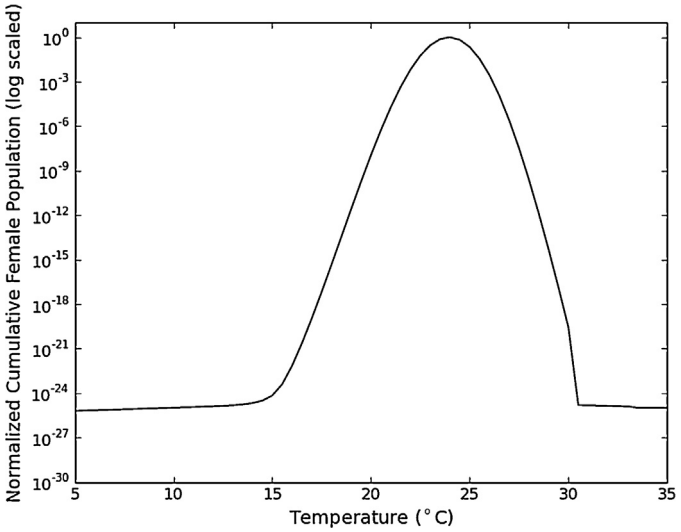

Fig. 5. Normalized cumulative female population for various constant temperatures. Simulations are 365 time steps in length, begin with 10 fecund females and do not include the diapause or fruit quality submodels.

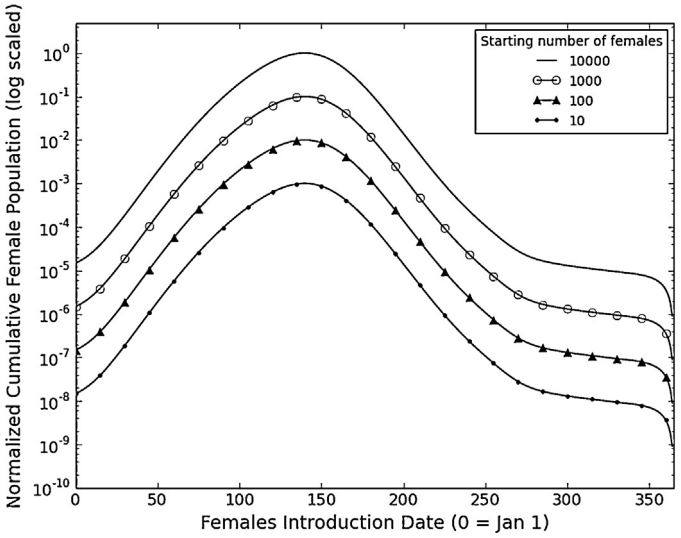

Fig. 6. Cumulative population sizes for varied initial introduction dates and populations sizes. In both cases, introduced flies are fecund females and the simulated timeframe uses model temperature profile Temp B. Individual simulations were run for 365 time steps.

appear in a region (Fig. 6). This sensitivity test does not consider the diapause and fruit quality submodels introduced later. The initial population size was varied from 10 to 10000 F_1 females, and the day on which they are added to the simulation was varied from 0 (i.e. January 1st) through 364 (December 31st). Model temperature profile Temp B (see Table 2) is shown here for illustration. Fig. 6 illustrates the resulting normalized cumulative population (all life stages) for different introduction dates and populations sizes.

Due to the continuous population representation and a single introduction date, the time step at which the population is introduced has a strong impact on the cumulative population size. For very early introduction dates the population can become extremely small despite having the maximum potential time for growth. Increased mortality as well as decreased development at colder temperatures produces a decline in the population below one individual and tending towards (but not reaching) zero during the colder first part of the simulated year. This creates a population 'deficit' that must then be overcome during the warmer periods. As the initial appearance day occurs later in the year this effect lessens and cumulative population increases significantly. In general this increase continues until the maximum cumulative population occurs with an introduction date that avoids decline due to early cold and allows for maximum time for the population to increase before temperatures decrease later in the year. In this simulation the optimal appearance day was May 21st. After this date the cumulative population decreases as declining temperatures in the fall and winter leave the population with less opportunity for positive growth. The optimal date of introduction is dependent on the location-specific yearly temperature profile, and is affected by the rate at which temperatures increase as well as the maximum temperatures which, when above heat tolerance, affect mortality and male sterility. Simulations run with temperature profiles that have less pronounced seasonality (regardless of peak temperature) are less sensitive to introduction date. Varying the starting population has a direct linear scaling effect on the cumulative population for a given introduction date.

3.3. Diapause submodel

As stated in Section 1, the precise environmental control on diapause induction is not yet known for this species of *Drosophila*, but we made the reasonable assumption that it is similar to that found for other species of *Drosophila*. Sensitivity analysis of the diapause submodel suggests that the number of daylight hours required to induce diapause has little effect on the cumulative population size (see Supplemental Fig. S2). This is due to the fact that temperatures decline and population growth rates decrease before diapause induction actually occurs. Because of this minimal effect, the diapause induction parameter was fixed at a conservative 10 h of daylight for all simulations.

Similarly, the precise temperature causing diapause termination is not yet known for this species. Based on work for other species of *Drosophila*, we estimated that 18 °C was a reasonable first approximation for this parameter value. We investigated the impact of diapause termination temperature on the cumulative population for all four model temperature profiles (Fig. 7).

Unlike the number of daylight hours required for diapause induction, temperature-based diapause termination does have a large effect on the cumulative population. In particular, as the termination threshold temperature increases, the amount of time available for population growth is reduced, and thus the cumulative population size declines. It is worth noting that the effect of diapause is most noticeable in regions of moderate climate (i.e., Temp profile C). In regions where temperatures are warm and relatively constant throughout the year (Temp D), the population is less sensitive to this parameter, as the higher temperatures ensure that the population breaks diapause early and cumulative population size is maximized. Only when the diapause termination temperature is set to unrealistically high values does it affect the population. In cooler climates (Temp A and B) the effect of diapause termination is also minor as the temperatures do not reach the diapause threshold until well into the year and the temperature profile is not as favourable for population growth when diapause is broken.

As discussed previously (Fig. 6), the introduction of the initial flies when temperatures are too cool to promote positive development can cause a population deficit that may not be overcome, particularly when the diapause termination threshold is high relative to local warm season temperatures. This population deficit is biologically unrealistic and in order to correct for this the initial individuals are added on the timestep when the temperature is adequate to break diapause. Fig. 8 shows the combined effects of the base population dynamics and diapause submodel with various modelled temperature profiles.

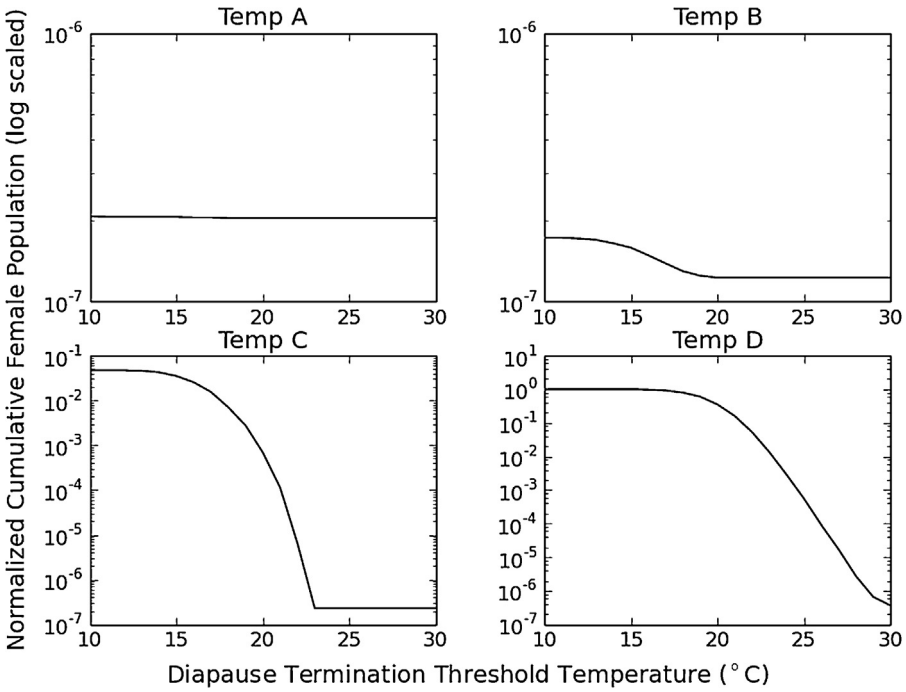

Fig. 7. The effect of diapause termination temperature on cumulative populations for model temperature profiles Temp A through D. Each simulation starts with 10 fecund females introduced into the simulation at time step 0 and was run for 365 days. Diapause induction is fixed at 10 h of daylight for all simulations. Note the difference in the *y*-axis scaling between graphs.

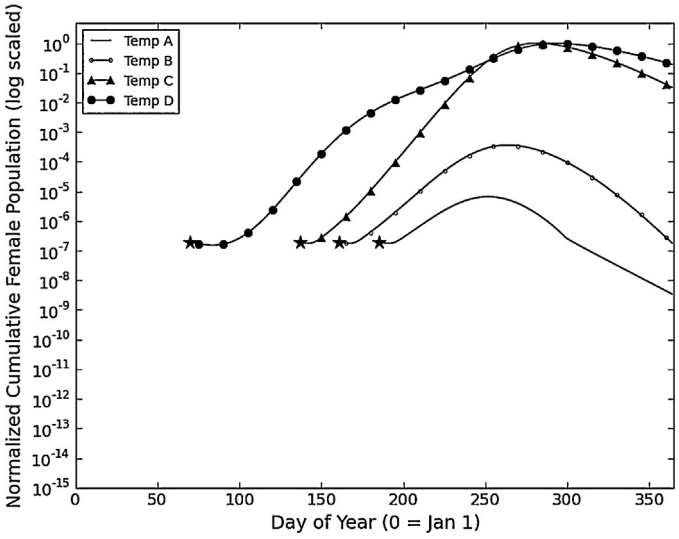

Fig. 8. Normalized per-day female count for each of the model temperature profiles. 10 fecund females are introduced into the simulation on the time step (starred) for which diapause would be terminated due to adequate temperature.

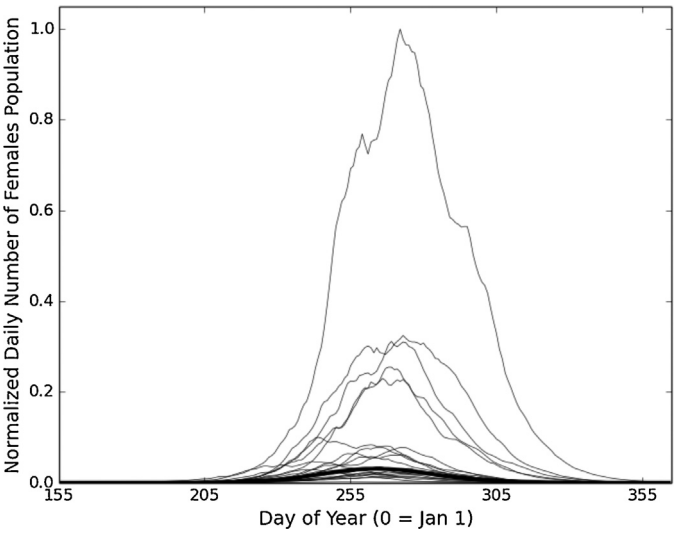

Fig. 9. Normalized per-day female (all adult stages) population dynamics using observed daily mean temperature data for Clark County, WA (1993–2013). Bold line indicates simulation using 20 year average daily temperature. 10 females are introduced into the simulation on the time step where temperature is adequate to break diapause.

Each of the illustrated populations shows similar growth followed by decline after peak temperature. Temp D has the earliest diapause termination date due to warmer temperatures earlier in the model year. The population increases quickly but the rate slows somewhat as temperatures exceed those required for optimal development. Temp C produces a later diapause termination date but surpasses the population size of Temp D as it remains at or near optimal development temperatures for a longer period. Temp A produces the lowest population peak due to the latest diapause termination date and temperatures consistently below optimal development.

3.4. Observed temperature data simulations

In addition to the cosine temperature curves, we also used observed daily mean temperature records, and 20-year average daily temperature as a way of investigating the influence of interannual variability and climate. Fig. 9 illustrates the population dynamics based on empirical temperature data. We conducted 21 separate simulations, 20 using observed daily average temperature for Clark County WA from 1993 to 2013 inclusive, and one using the 20-year averaged daily temperatures. The results show the normalized daily count of females (all stages).

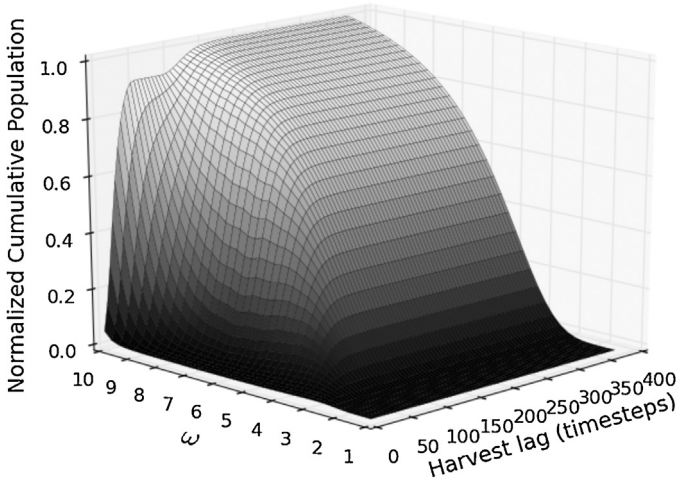

Fig. 10. Fruit submodel effect on cumulative population. Simulations start with 10 fecund females introduced on time step 75 and are run for a duration of 365 time steps. Model temperature profile Temp B is used. Cumulative population is maximized as both ω (the quality rate limiter) and harvest lag increase resulting in optimal food availability for the simulated population.

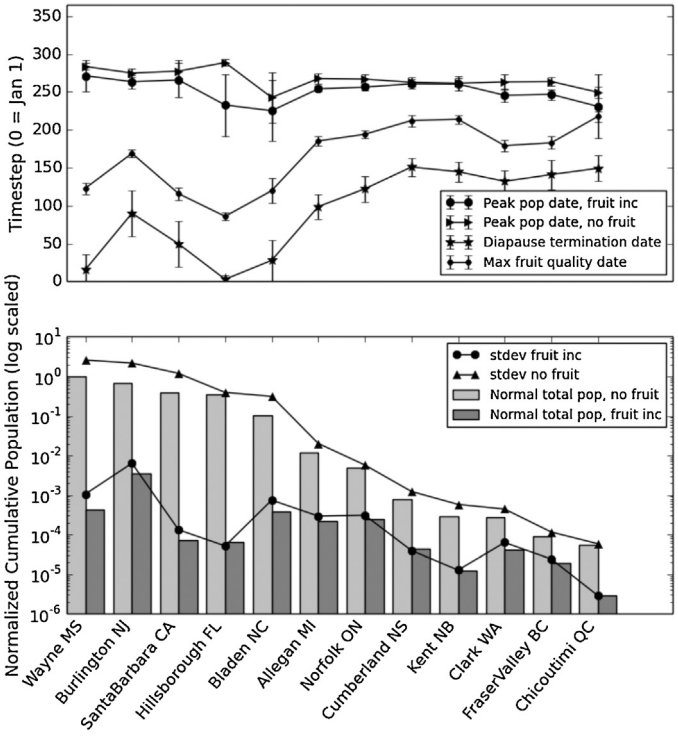

Fig. 11. Population dynamics, including diapause and fruit quality considerations, for various soft-skin fruit producing counties and townships across the United States and Canada. Cumulative population is normalized to show relative potential population sizes. Time step at which diapause would terminate and peak adult female population occurs for the diapause-only and diapause-fruit models are also shown. Locations are sorted by latitude (low to high).

These results illustrate the flies' sensitivity to annual variation in temperature. We can look to several temperature cues to highlight the reasons for the large spread of values. The mean annual temperature for the year producing the largest population (2003) is 12.0 °C (the second largest mean daily temperature of the 20-year data set) compared with 10.84 °C for the year producing the smallest peak population (1996). In addition, diapause terminates on April 8th in 1996 and on May 23rd in 2003. While this would appear to give the 1996 population a 45-day growth advantage, instead diapause terminates on an abnormally warm day early in the year and subsequently the population crashes when temperatures return to low seasonal norms. The later diapause termination date in 2003 ensures that the population begins and maintains a positive growth phase at a near-optimal time step for population growth. Comparing the 2003 population with that of 2004, which has the highest annual average daily temperature at 12.14 °C, we note that 2004 has the fourth highest cumulative population, approximately one third that of 2003. Again we find that an earlier diapause termination on April 27th results in a short phase of negative population growth followed by sub-optimal positive growth early in the simulation compared to the optimal growth of the 2003 population. Diapause termination date and mean daily temperature together contribute significantly to the cumulative population size.

3.5. Fruit submodel

Up to this point, we have illustrated the behaviour of the model under the assumption that food is always available at an optimal quality for development. Fig. 10 shows the effect on the cumulative population of varying the quality of available food through the fruit submodel. For these simulations 10 F_1 females were introduced on March 16th (day 75) rather than at diapause termination as the diapause submodel was not considered for these simulations. The ω multiplier determines the rate at which fruit reaches optimal quality and the harvest lag determines the number of days in which optimal quality fruit will be available to the simulated population. The simulations were run for the temperature profile Temp B.

We note that as ω increases so too does the population as fruit becomes available ealier in the year, thereby optimizing the opportunity for population growth. This effect is enhanced when the harvest lag increases, but only until the lag reaches approximately 100 days, after which factors such as temperature-driven mortality and late-year declining temperature and diapause initiation determine population thresholds. The effect of the fruit submodel is similar for various locations tested but it is worth noting that with a fixed ω muliplier optimal fruit quality is reached sooner in regions with warmer temperatures while in regions with colder temperatures may not be reached at all preventing the population from reaching its maximum potential size. Furthermore, a short harvest lag time can inhibit population growth by limiting food source availability. This effect is most pronounced when ω is very low (late ripening fruit) or very high (early ripening fruit) and when combined with a short harvest lag period.

3.6. The complete model

The complete model combines the effects of diapause and the fruit submodel. In Fig. 11 we illustrate the complete model's behaviour. Normalized cumulative populations are shown for various strawberry and blueberry producing counties in the United States and townships in Canada For each location daily average temperature data were obtained for the years 1993 through 2013. The simulation was run for 365 days and the mean normalized cumulative population, diapause termination date and date at which the peak number of adult females occurred were recorded for each year for each location. To illustrate the effects of the fruit quality submodel, the simulations are repeated with the same parameters and temperature data and the fruit parameters ω set to 4.0 and harvest lag time set to 50 days. Also included are the dates where peak population (adult females) occurs for the model both including and excluding the fruit submodel.

In the simulation without the fruit quality submodel it is the southern-most counties that produce the largest simulated populations of *D. suzukii*. The relatively northern Burlington County,

New Jersey appears to be an exception to this primarily due to warmer, but not extreme, temperatures throughout the year. The maximum temperature-based intrinsic mortality and upper threshold for temperature-based development are reached at 33 °C and 31 °C respectively, which explains why a region with more moderate temperatures such as Burlington county might have one of the larger populations. If the temperatures are near optimal for development (approximately 24 °C) with minimal days above the threshold for maximum mortality or minimum development, then a population could grow optimally at a more northern latitude. The diapause termination date follows a largely south-to-north trend due to higher temperatures early in the year. However, there is little evidence of a significant lattitudinal trend for peak population date due to a combination of declining temperatures and diapause induction in all locations later in the year.

Since the base model implies that food is available at optimal quality at all times smaller overall populations were observed when the fruit quality submodel was included (Fig. 9). Because development decreases and mortality increases when fruit is not at optimal ripeness, populations do not reach the maximums observed when the fruit submodel is not present. Peak population size is reached earlier in the year when the fruit submodel is included. This is the result of a decline in population after the harvest lag time has elapsed. When the fruit submodel is ignored populations can continue to grow provided diapause has not been initiated and temperatures are favourable. The warmer regions in Hillsborough (FL), Santa Barbara (CA) and Wayne (MS) have lower cumulative populations than might be expected since the fruit in the model, also being temperature dependent, ripens very quickly. The population then grows optimally for the duration of the harvest lag time after which development rates decrease due to the limited availability of fruit for the remainder of the simulated year. On the other hand, regions where the fruit grows more slowly offer the population a sub-optimal quality yet available food source for a longer period of time followed by the same harvest lag time thus producing relatively larger populations.

3.7. Extrinsic mortality

Extrinsic mortality (i.e. mortality due to predators, parasites and pathogens) in the field is inherently difficult to quantify but is likely a very important determinant of population size. The simulations shown in Fig. 11 considered extrinsic mortality to be zero. Here we show the impact that increasing extrinsic mortality has on relative population size (Fig. 12). We can see that as extrinsic mortality approaches intrinsic mortality in magnitude (i.e. total mortality is doubled), the resulting population size declines by nearly four orders of magnitude.

These results indicate that extrinsic mortality can potentially be a major factor in determining population size. We modelled extrinsic mortality as always being *additional* to intrinsic mortality. That is, we assume that extrinsic mortality never compensates for intrinsic mortality. This may or may not be a good assumption, and this will be explored further in subsequent work. In any case, this result highlights the need to obtain estimates of this rate if we are to accurately predict the population dynamics for this species.

4. Discussion

The population dynamics model presented herein has been developed using known life history traits of *D. suzukii* and is consistent with empirical data and known mechanistic responses to air temperature (Ryan et al., 2016, Emiljanowicz et al., 2014; Tochen et al., 2014; Kinjo and Kunimi, 2014). Temperatures that remain well below those required for optimal development produce relatively small populations due to a prolonged development period, reduced fecundity and increased intrinsic mortality. Temperatures that peak above the optimal development temperature, and that remain high, also have a negative impact on population size due to an increase in temperature-dependent mortality and reduced development rate, while ideal temperature profiles remain within a few degrees of optimal temperature for development. As expected, cumulative population numbers varied by region, often by several orders of magnitude, depending on regional temperature profiles.

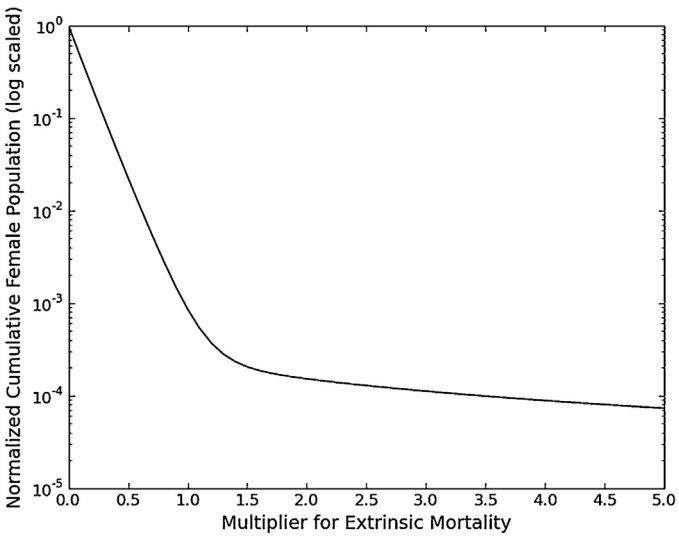

Fig. 12. The effect of increasing extrinsic mortality in proportion to intrinsic mortality. As the extrinsic mortality increases, the cumulative population decreases.

We also considered the effects of diapause on population responses. Photoperiod-induced diapause has been characterized in numerous Drosophilid species (Kimura, 1990; Lumme et al., 1974; Salminen et al., 2012; Saunders et al., 1989). For example in *D. melanogaster* newly eclosed females undergo diapause when exposed to short days (<14 h of light); photoperiod-induced diapause is then terminated rapidly by transfer to 18 °C (Saunders et al., 1989). However, there is relatively little information on diapause in *D. suzukii*. Ryan et al. (2016) found that pre-exposure to short photoperiod (10:14 L:D) had no effect on the survival responses of adult *D. suzukii* to long-duration low-temperature exposure relative to controls (15:9 L:D), however the level of ovarian maturation in that study was unknown, and as such it was not clear if short photoperiod induced physiological diapause. Jakobs et al. (2015) also found no evidence of diapause in *D. suzukii* following two weeks of exposure to simulated fall conditions, though while photoperiod may have been short enough to induce diapause (11.5:12.5, and 12:12 L:D), daytime temperatures in that study were relatively high during this exposure (9/21 °C and 5.5/19 °C). Consequently, the diapause submodel presented here is both simplified and generalized due to a lack of specific detail on *D. suzukii* diapause characteristics, but could easily be refined as data become available.

Our diapause sensitivity analysis suggests that diapause termination temperature is more important for population growth than the photoperiod at which diapause is induced. This is because low fall temperatures have a strong negative impact on development and fecundity in advance of diapause induction. Empirical observations of *D. suzukii* temperature-dependent development show that fall temperatures substantially slow development. Ryan et al. (2016) found that egg-to-adult development of *D. suzukii* took 30.3 days at 15 °C, 75.1 days at 10 °C and was suspended at temperatures of 8 °C and below. Similar results for *D. Suzukii* have also been found by Tochen et al. (2014). As such, in many cases devel-

opment had slowed or stopped in the current model in advance of diapause induction. However, temperature-based diapause termination could significantly impact overall population size with early diapause termination, coupled with consistently warm temperatures, representing ideal conditions for population growth. Moderate climates are the most sensitive to termination temperature, while areas with warm temperatures are less sensitive to this parameter, as the higher temperatures ensure that the population breaks diapause early and cumulative population size is maximized (Fig. 7). These runs were performed with mathematically generated temperature profiles however, and the behaviour is likely to be different in reality, where temperatures are fluctuating. For example, in cases where diapause breaks early because of transient unseasonably high temperatures, populations may be at a disadvantage once temperatures return to lower seasonal norms (Fig. 6). Fluctuating temperatures have also been shown to alter temperature-dependent life history traits. For example, *D. melanogaster* reared under fluctuating-temperature conditions had a higher tolerance to both heat and cold than those exposed to constant temperatures (Overgaard et al., 2011).

Our analysis of the sensitivity of the model to the initial number of individuals demonstrates that the peak population predictably scales with the initial number of females (Fig. 6). This highlights the importance of overwintering survival to the final population size. However, the model is limited to single-year simulations due to a lack of available data on the overwintering of *D. suzukii*, though some progress has been made in this area. It is now known that *D. suzukii* are chill-susceptible and are likely to have low survival in regions that experience low winter temperatures. Jakobs et al. (2015) found that 80% of flies were killed after 1 h at −7.2 °C for males, and −7.5 °C for females. Additionally, it was found that populations in field cages in Southern Ontario were killed early in the winter by a transient cold snap (Jakobs et al., 2015). This would suggest that in severe winters, where temperatures regularly fall below zero, spring populations of *D. suzukii* are likely due to new migrations or from populations overwintering in human-made structures. As data are collected on overwintering, immigration, invasion and transportation characteristics, the model may be enhanced to produce multi-year simulations with carry-over of individuals between years. Further, for many regions humidity is also likely be an important characteristic for development fecundity and mortality (Tochen et al., 2015) but is not considered here.

The current model also illustrates the impact of fruit quality on population size. Fruit of high quality and availability can, in conjunction with environmental factors, optimize population growth while lower quality fruit (pre-ripened) and low availability (post-harvest) are likely to have a negative impact. The fruit quality submodel presented here is simplified and represents no specific fruit development model though it is general enough that it may be parameterized for specific hosts for which development data are available. Fig. 11 illustrates the effects of host availability on population size and shows that unlimited availability of appropriate hosts can result in cumulative population numbers that are several orders of magnitude higher than situations where food is transiently available. *D. suzukii* have many known non-crop hosts that may grow in field margins, hedgerows, or areas with unmanaged woody or riparian ornamentals, shrubs or vines that are able to sustain *D. suzukii* populations (Lee et al., 2015). As such, *D. suzukii* populations in crops are likely heavily influenced by the availability of wild hosts between harvests. The impact of fruit availability on population numbers therefore strongly argues for management practices that include cultural controls such as removal of wild hosts and destruction of rotting fruit post-harvest.

Wiman et al. (2014) have produced a model to explore *D. suzukii* population dynamics with several similarities to the model presented here. Both models incorporate environmental factors, particularly temperature, to determine survival and fecundity, both assume that food is always available to the population and both minimize early-year negative population growth using roughly analogous 'biofix' (Wiman et al., 2014) and diapause termination. There are however, important differences. The Wiman model is based on Leslie matrices and is thus a discrete time model, and critical population parameters are based on the empirical observations of Tochen et al. (2014). In contrast, our model is continuous in time representation and is based primarily on experiments conducted by our group (Emiljanowicz et al., 2014; Ryan et al., 2016). While the observations of Tochen et al. and Ryan et al. are similar, experimental changes such as fruit versus artificial diet (respectively) may account for discrepancies in the resulting parameters which may in turn be reflected in the differing results between the two models. Finally, we have included a diapause submodel whereas diapause appears to be considered only during the calculation of the initial population size in the Wiman model. When the diapause and fruit submodels are included the difference in resultant population size between the two models (Supplemental Fig. S6) are amplified as our model shows a sharper decline in population in the later months due largely to the induction of diapause and the decrease in fruit quality.

Another recent model is that of Gutierrez and Ponti (cf. Asplen et al., 2015, Supplementary material). They present a physiologically-based demographic model (PBDM) parameterized with development and mortality rates based on the data of Tochen et al. (2014), Dalton et al. (2011), and Kinjo and Kunimi (2014) as well as unpublished laboratory data. The model is stage specific including egg, larval, pupal and adult stages. Although an explicit diapause phase is not included, a reproductive quiescence is initiated when food hosts are unavailable (due to low temperatures) or temperatures are considered too low to support reproduction. Unlike the model presented here, Gutierrez and Ponti include consideration for relative humidity on fecundity and overwintering of reproductively quiescent adults. Despite the differences many of the conclusions remain the same; temperature and host availability are among the principle drivers of population size and as such warmer climates are likely to experience larger and potentially more destructive infestation than cooler climates. Taken together, the differences between the three models and their predictions help shape our understanding of how different abstractions add to our knowledge of population dynamics in this species.

Given that *D. suzukii* is a relatively new pest in North America, research is ongoing to establish its actual and potential impact on the soft-skinned fruit and berry industries (Goodhue et al., 2011; Bolda et al., 2010). Studies of the effectiveness on pesticides and information campaigns (Beers et al., 2011; Dreves 2011; Bruck et al., 2011; Walse et al., 2012) are already underway. It is important to acknowledge the cost of these measures, both financial and environmental, and that fruit-growing regions are not at equal risk for significant loss due to infestation. In some areas environmental factors may prohibit *D. suzukii* from reaching the required critical mass and might avoid costly chemical treatments. In other areas such treatments may be routinely unavoidable. However, inter-annual fluctuations in temperature and longer-term climate change may cause *D. suzukii* population levels to change, which may require appropriate adjustments in management strategies. As further field and laboratory data becomes available models such as the one presented here will continue to add important insights and may be considered important tools for stakeholders looking to prevent or mitigate the effects of *D. suzukii* in high risk regions. Furthermore as the global climate changes relative risk may also change on a regional basis. Areas of low risk due to temperate summers and colder winters may become more hospitable as temperatures rise while currently high risk areas may experience reduced *D. suzukii* presence due to an increase of temperature outside of developmen-

tal or mortality range. Regional cooling on a shorter time scale as climate shifts occur may also have an impact on the presence and impact of *D. suzukii*. These climate impacts are an important area of study when considering a long-term strategy for managing this species (Langille et al., unpublished).

Acknowledgements

This research was supported by grants from the Ontario Ministry of Agriculture, Food and Rural Affairs (OMAFRA) and the Canadian Natural Sciences and Engineering Research Council (NSERC) to JAN. The authors would also like to thank Nik Wiman et al. for providing data and the permission to replicate it in this work, as well as Steven Zarichney for assistance with GIS.

Appendix A. Supplementary data

Supplementary data associated with this article can be found, in the online version, at http://dx.doi.org/10.1016/j.ecolmodel.2016.05.014.

References

Asplen, M.K., Anfora, G., Biondi, A., Choi, D.S., Chu, D., Daane, K.M., Desneux, N., 2015. Invasion biology of spotted wing drosophila (*Drosophila suzukii*): a global perspective and future priorities. J. Pest Sci. 88 (3), 469–494, http://dx.doi.org/10.1007/s10340-015-0681-z.

Beers, E.H., Van Steenwyk, R.A., Shearer, P.W., Coates, W.W., Grant, J.A., 2011. Developing *Drosophila suzukii* management programs for sweet cherry in the western United States. Pest Manag. Sci. 67 (11), 1386–1395.

Bolda, M.P., Goodhue, R.E., Zalom, F.G., 2010. Spotted Wing Drosophila: Potential Economic Impact of a Newly Established Pest, 13(3. Agricultural Resource Economics. Update. University of California Giannini Foundation of Agricultural Economics, pp. 5–8.

Briere, J.-F., Pracros, P., Le Roux, A.-Y., Pierre, J.-S., 1999. A Novel rate model of temperature-dependent development for arthropods. Environ. Entomol. 28 (1), 22–29.

Bruck, D.J., Bolda, M., Tanigoshi, L., Klick, J., Kleiber, J., DeFrancesco, J., Gerdeman, B., Spitler, H., 2011. Laboratory and field comparisons of insecticides to reduce infestation of *Drosophila suzukii* in berry crops. Pest Manag. Sci. 67 (11), 1375–1385.

Burrack, H.J., Fernandez, G.E., Spivey, T., Kraus, D.A., 2013. Variation in selection and utilization of host crops in the field and laboratory by *Drosophila suzukii* Matsumara (Diptera: Drosophilidae), an invasive frugivore. Pest Manag. Sci. 69 (10), 1173–1180.

Dalton, D.T., Walton, V.M., Shearer, P.W., Walsh, D.B., Caprile, J., Isaacs, R., 2011. Laboratory survival of *Drosophila suzukii* under simulated winter conditions of the Pacific Northwest and seasonal field trapping in five primary regions of small and stone fruit production in the United States. Pest Manag. Sci. 67 (11), 1368–1374.

Dreves, A.J., 2011. IPM program development for an invasive pest: coordination, outreach and evaluation. Pest Manag. Sci. 67 (11), 1403–1410.

Emiljanowicz, L.M., Ryan, G.D., Langille, A., Newman, J., 2014. Development, reproductive output and population growth of the fruit fly pest *Drosophila suzukii* (Diptera: Drosophilidae) on artificial diet. J. Econ. Entomol. 107 (4), 1392–1398.

Glarner, H., 2006. Length of Day and Twilight (January 15), Retrieved from http://www.gandraxa.com/length_of_day.xml.

Goodhue, R.E., Bolda, M., Farnsworth, D., Williams, J.C., Zalom, F.G., 2011. Spotted wing drosophila infestation of California strawberries and raspberries: economic analysis of potential revenue losses and control costs. Pest Manag. Sci. 67 (11), 1396–1402.

Hauser, M., 2011. A historic account of the invasion of *Drosophila suzukii* (Matsumura) (Diptera: Drosophilidae) in the continental United States, with remarks on their identification. Pest Manag. Sci. 67 (11), 1352–1357.

Jakobs, R., Gariepy, T.D., Sinclair, B.J., 2015. Adult plasticity of cold tolerance in a continental-temperate population of *Drosophila suzukii*. J.Insect Physiol. 79, 1–9.

Kanzawa, T., 1939. Studies on *Drosophila suzukii* Mats. Kofu. Rev. Appl. Entomol. 29, 622.

Kimura, M.T., 1990. Quantitative response to photoperiod during reproductive diapause in the *Drosophila auraria* species-complex. J. Insect Physiol. 36 (3), 147–152.

Kinjo, H., Kunimi, Y., 2014. Effects of temperature on the reproduction and development of *Drosophila suzukii* (Diptera: Drosophilidae). Appl. Entomol. Zool. 49, 297–304.

Lee, J.C., Bruck, D.J., Curry, H., Edwards, D., Haviland, D.R., Van Steenwyk, R.A., Yorgey, B.M., 2011. The susceptibility of small fruits and cherries to the spotted-wing drosophila, *Drosophila suzukii*. Pest Manag. Sci. 67 (11), 1358–1367.

Lee, J.C., Dreves, A.J., Cave, A.M., Kawai, S., Isaacs, R., Miller, J.C., Van Timmeren, S., Bruck, D.J., 2015. Infestation of wild and ornamental noncrop fruits by *Drosophila suzukii* (Diptera: Drosophilidae). Ann. Entomol. Soc. Am. 108 (2), 117–129.

Lumme, J., Oikarinen, A., Lakovaara, S., Alatalo, R., 1974. The environmental regulation of adult diapause in *Drosophila littoralis*. J. Insect Physiol. 20, 2023–2033.

Mitsui, H., Beppu, K., Kimura, M.T., 2010. Seasonal life cycles and resource uses of flower- and fruit-feeding drosophilid flies (Diptera: Drosophilidae) in central Japan. Entomol. Sci. 13 (1), 60–67.

Newman, J.A., Gibson, D.J., Parsons, A.J., Thornley, J.H.M., 2003. How predictable are aphid population responses to elevated CO_2? J. Anim. Ecol. 72 (4), 556–566.

Ohtsu, T., Katagiri, C., Kimura, M.T., Hori, S.H., 1993. Cold adaptations in *Drosophila*: qualitative changes of triacylglycerols with relation to overwintering. J. Biol. Chem. 268, 1830–1834.

Overgaard, J., Hoffman, A.A., Kristensen, T.N., 2011. Assessing population and environmental effects om thermal resistance in *Drosophila melanogaster* using ecologically relevant assays. J. Therm. Biol. 36, 409–416.

Ryan, G.D., Emiljanowicz, L.M., Wilkinson, F., Kornya, M., Newman, J.A., 2016. Thermal tolerances of the spotted wing drosophila *Drosophila suzukii*. J. Econ. Entomol., http://dx.doi.org/10.1093/jee/tow006 http://jee.oxfordjournals.org/content/109/2/746.

Salminen, T.S., Vesala, L., Hoikkala, A., 2012. Photoperiodic regulation of life-history traits before and after eclosion: egg-to-adult development time, juvenile body mass and reproductive diapause in *Drosophila montana*. J. Insect Physiol. 58, 1541–1547.

Saryazdi, S., Cheriet, M., 2007. PKCS: a polynomial kernel family with compact support for scale—space image processing. IEEE Trans. Image Process. 16 (9), 2299–2308.

Saunders, D.S., Henrich, V.C., Gilbert, L.I., 1989. Induction of diapause in *Drosophila melanogaster*: photoperiodic regulation and the impact of arrhythmic clock mutations on time measurement. Proc. Natl. Acad. Sci. U. S. A. 86 (10), 3748–3752.

Stephens, A.R., Asplen, M.K., Hutchison, W.D., Venette, R.C., 2015. Cold hardiness of winter-acclimated *Drosophila suzukii* (Diptera: Drosophilidae) adults. Environ. Entomol., http://dx.doi.org/10.1093/ee/nvv134.

Thornley, J.H.M., France, J., 2007. Mathematical Models in Agriculture: Quantitative Methods for the Plant, Animal and Ecological Sciences, 2nd edition. CABI, Wallingford, UK.

Tochen, S., Dalton, D.T., Wiman, N., Hamm, C., Shearer, P.W., Walton, V.M., 2014. Temperature-related development and population parameters for *Drosophila suzukii* (Diptera: Drosophilidae) on cherry and blueberry. Environ. Entomol. 43 (2), 501–510.

Tochen, S., Woltz, J.M., Dalton, D.T., Lee, J.C., Wiman, N.G., Walton, V.M., 2015. Humidity affects populations of *Drosophila suzukii* (Diptera: Drosophilidae) in blueberry. J. Appl. Entomol., http://dx.doi.org/10.1111/jen.12247.

Walse, S.S., Krugner, R., Tebbets, J.S., 2012. Postharvest treatment of strawberries with methyl bromide to control spotted wing drosophila, *Drosophila suzukii*. J. Asia Pacif. Entomol. 15 (3), 451–456.

Walsh, D.B., Bolda, M.P., Goodhue, R.E., Dreves, A.J., Lee, J., Bruck, D.J., Walton, V.M., O'Neal, S.D., Zalom, F.G., 2011. *Drosophila suzukii* (Diptera: Drosophilidae): invasive pest of ripening soft fruit expanding its geographic range and damage potential. J. Integr. Pest Manag. 2 (1), G1–G7.

Wiman, N.G., Walton, V.M., Dalton, D.T., Anfora, G., Burrack, H.J., et al., 2014. Integrating temperature-dependent life table data into a matrix projection model for *Drosophila suzukii* population estimation. PLoS One 9 (9), e106909.

Zavalloni, C., Andresen, J.A., Flore, J.A., 2006. Phenological models of flower bud stages and fruit growth of 'Montmorency' sour cherry based on growing degree-day accumulation. J. Am. Soc. Hortic. Sci. 131 (5), 601–607.